Soil Water Content Measurement using Polymer Optical Fibre Bragg Gratings

Moura Mehravar (corresponding author), BSc, MSc, PhD

College of Engineering and Physical Science, Aston University, Birmingham, UK

Email: m.mehravar@aston.ac.uk

Hanrui Yang, BSc, MSc, PhD

School of Automation Engineering, Northeast Electric Power University, Jilin, China

Email: Yanghanrui@163.com

David J Webb, BA, PhD

College of Engineering and Physical Science, Aston University, Birmingham, UK

Email: D.J.Webb@aston.ac.uk

Wei Zhang, BSc, MSc, PhD
School of Aerospace, Transport, and Manufacturing, Cranfield University, Cranfield, UK
Email: Zhang.wei@cranfield.ac.uk

Sina Fadaie Sestelani, BSc, MSc
College of Engineering and Physical Science, Aston University, Birmingham, UK

Email: 200208408@aston.ac.uk

David N Chapman, BSc, PhD
School of Engineering, University of Birmingham, UK
Email: D.N.Chapman@bham.ac.uk

Abstract

Measuring soil water content is crucially important and can affect soil strength which is a key parameter in analysis, design and monitoring of geo-structures. In this study, an optical fibre Bragg grating (FBG) sensor inscribed in Polymer Optical Fibre (POF) was developed and for the first time its ability to measure soil water content was investigated. The sensitivity of the sensor to different values of gravimetric soil water content under different compaction conditions of loose and normal compaction was tested. The effect of soil temperature on the sensor's performance was considered. To assess the sensor's implementation, accuracy and reliability, a commercial soil water content probe (SM150), which measures volumetric soil water content was employed. The results indicate that the developed sensor when calibrated correctly, is able to provide detailed data on any minor variation of soil water content (e.g. 0.5%) with high precision. The outcomes of this study define an additional capability of the POFBG sensors which is significantly important for long-term performance monitoring of geo-structures.

Keywords: ground condition monitoring, gravimetric soil water content, polymer optical fibre Bragg grating (POFBG) sensor, geostructures

1. Introduction

The performance and health condition of geotechnical assets such as retaining walls, pavements' subbase layers, embankments, cuttings, flood levees, slopes and earth dams are considerably important in both developed and developing societies. Precise

prediction of the remaining service-life of these assets can assist with taking the most suitable engineering intervention to avoid/eliminate catastrophic failures. As such, it is important to improve our understanding of the current condition of existing (often aging) infrastructure (Soga, et al., 2015).

Generally, any failure or any condition which may cause failure in geo-structures, as well as their supporting ground, could potentially result in substantial damage to the infrastructure and disruption to their serviceability, and subsequently could affect society's function (Curioni, et al., 2018 a), (Du, et al., 2016), (Clarke, et al., 2017).

Changes in environmental (e.g. temperature and rainfall) and loading conditions alter soil properties including its mechanical properties and, in some circumstances, this can lead to permanent changes of the ground. Soil is a multi-phase material, typically made of solid soil particles, water and air, with water significantly governing its behaviour. Variations in soil water content due to global climate change (e.g. extreme wet and dry weather cycles), seasonal fluctuations, or local site changes such as leakage from utility pipes, will affect the strength and mechanical properties of soil leading to soil volume changes (shrink/swell mechanism) in fine grained soils. Hence, measuring soil water content is of critical importance to evaluate soil strength, which is an important parameter in the analysis, design and monitoring of geo-structures. Often very small changes in the soil water content over time can lead to collapse of the ground and any supported infrastructure resulting in damages and deterioration to our assets (Pritchard, et al., 2014), (Gunn, 2015). Examples of such events are land sliding, collapse of expansive clays, and sinkholes. Additionally, several studies have shown that the soil water content has a significant effect on roads' and railways' subgrade performance (Bryson, et al., 2012). In other words, strength and deformation of subgrade materials are directly associated with the soil water content, hence this

parameter must be accurately measured and monitored during construction and service life of geo-structures (Mitchell & Soga, 2005).

In general, due to the complex, multi-phase, anisotropic and non-homogenous nature of soils, the accurate measurement of their water content in the field is one of the greatest challenges that geotechnical engineers face during the site investigation stage of ground works as well as assessment and monitoring the condition of geo-structures during their service life.

The soil water content (sometimes known as moisture content) is expressed as either gravimetric basis (w) or volumetric basis (θ). Soil gravimetric water content, w, is calculated as ratio of mass of the water contents to mass of solid particles whilst volumetric water content, θ, is defined as volume of water over total volume in any given sample. For almost all basic relationships and calculations that are relevant to the strengths of soils in geotechnical engineering, the gravimetric variant is the preferred format as it can be accurately measured in the laboratory by the oven-drying method (BSI, 1999 (a)) and can be directly used to describe the mechanical behaviour of the soil (Curioni, et al., 2018 b). Volumetric and gravimetric soil water content and their relationship can be expressed by Equations 1a-1c.

$$w = \frac{m_w}{m_s} \tag{1a}$$

$$\theta = \frac{V_w}{V} \tag{1b}$$

$$\theta = w\,\frac{\rho_d}{\rho_w} \tag{1c}$$

Where m_w is mass of water; m_s is mass of soil (solid particles) in the sample; V_w is volume of a soil mass which is occupied by water (m^3); V is total volume of soil being investigated; ρ_d is soil dry density; and ρ_w is density of the water.

In order to measure the soil water content, several different electrical sensors and cable systems have been developed, some of which are for use in the field, to monitor geo-structures. Often, these sensors are calibrated to measure volumetric water content i.e. θ (Robinson, et al., 2008). They are exposed to harsh environmental conditions (Huang Chien, et al., 2016) and therefore, the signal stability as well as system durability of the monitoring system are significantly important. Of available geophysical techniques, most notably is the time domain reflectometry or TDR (an electro-magnetic -based method) that is used to measure θ at point locations in the field. However, this method suffers from lack of accuracy, particularly at low moisture content, amongst other shortcomings, which limits its use (Curioni, et al., 2018 b). Other techniques such as neutron probe, or ground penetrating radar are costly and/or require expertise to set-up and interpret which may not be readily available (Robock, 2014). Additionally, they are limited to certain soil types or environmental conditions (Huisman, et al., 2003). The study reported in this paper explores the feasibility of using a novel type of fibre optic sensing technique that lies outside the conventional electrical techniques and therefore does not suffer from the above limitations.

Over the past 40 years, fibre optic sensors have established themselves as a mature technology in applications where their unique properties give them advantages (Byoungho, 2003). These advantages include low fibre loss (enabling operation over multi-kilometre distances without intermediate amplification), their dielectric nature (granting them immunity to electromagnetic interference), their small size (enabling embedding in smart materials) and the robust nature of silica, allowing them to be used

in harsh environments, e.g. at temperatures of several hundred °C. A particularly successful type of fibre optic sensor is the fibre Bragg grating (FBG). These take the form of a laser-inscribed periodic axial spatial modulation of the fibre core refractive index, which has the effect of reflecting back down the fibre light with a wavelength determined by the period of the modulation and the value of the core index. From a sensing perspective, it is important to note that the period of the modulation and the fibre core index are both affected by any strain or temperature change applied to the fibre, resulting in a shift in the back-reflected wavelength. Hence, by monitoring the light reflected by the FBG the strain or temperature of the fibre may be deduced.

Whilst the majority of optical fibres are fabricated from silica, recent years have witnessed the development of the technology of FBGs recorded in polymer optical fibre (Webb, 2015). A feature of one of the common polymers used – poly(methyl methacrylate) (PMMA) – is that it has an affinity for water, the absorption of which causes a swelling of the fibre and an increase in its refractive index, both of which contribute to a positive shift in the Bragg wavelength of any inscribed grating (Zhang & Webb, 2014). This is an equilibrium process where the amount of water absorbed by the fibre is determined by the degree of saturation of the fibre environment. The shift in the Bragg wavelength can therefore be used to determine the humidity of the air surrounding the fibre. The nominal response time for the equilibrium process of polymer optical fibre Bragg gratings to humidity tends to be a few tens of minutes and this does change considerably from fibre to fibre, which is related to the differing molecular weight distributions of the fibres however reduced-diameter (etched) fibres can have response times down to a few seconds (Rajan, et al., 2013).

Fibre optic sensors have been proposed for a number of geotechnical applications (Gong, et al., 2019). Mainly these have required the monitoring of strain, force or

movement, though a recent paper (Lopez Aldaba, et al., 2018) describes a soil moisture sensor based on a fibre Fabry-Perot interferometer formed in a short length of microstructured fibre coated with SnO_2.

The aim of this feasibility study was to assess the ability and accuracy of polymer optical fibre Bragg grating (POFBG) sensors as the basis for an effective, accurate and inexpensive approach for soil condition monitoring by measurement of gravimetric water content (w). For the first time, the sensitivity of a fibre Bragg grating (FBG) sensor fabricated in polymer optical fibre (POF) to soil water content changes was investigated. The sensor was tested at various values of gravimetric water content in different soil compaction conditions, and the obtained results were validated against traditional methods for soil water content measurement. Additionally, the effect of soil temperature on the sensor's response was considered and a temperature correction factor was determined.

2. Sensor fabrication and packaging

2.1 Polymer optical fibre Bragg gratings

Polymer optical fibre Bragg gratings (POFBGs) have been extensively studied and utilised in many application in the past 20 years and yet they also remain a topic of research, as people seek to exploit non-standard fibre types or develop new applications; an example of this is the development of grating technology in polymer optical fibres which have different measurand sensitivities compared to silica fibre (Webb, 2015).

Fibre Bragg gratings (FBGs) can be photo-inscribed in optical fibres made from a variety of polymers, including poly methyl methacrylate (PMMA), TOPAS, Zeonex, polycarbonate and CYTOP (Mehravar, et al., 2019). The physical properties of

polymers can obviously be very different to those of silica and this leads to FBG sensors in polymer fibre having rather different features to those in silica fibre. In particular, POFBGs can survive repeated straining in excess of 5% and even over 10%, depending on the fibre fabrication and drawing conditions. They have a lower elastic modulus compared to silica based FBGs so when POFBGs are strained, the tension in the fibre is typically 25 times less and so the sensor exerts much less influence on its surrounding medium – important when FBGs are being used to sense strain in compliant materials (Webb, 2015).

Polymer optical fibres (POFs) composed of PMMA have an affinity for water, which when absorbed by the fibre, causes a swelling accompanied by an increase in refractive index, both of which result in a shift of the Bragg wavelength to higher values. The water absorption is a reversible process with the amount of water in the fibre being determined by the equilibrium relative humidity in the region surrounding the fibre (Harbach, 2008). Considering the POFBG sensitivity to the relative humidity of its environment, this property also makes the POFBG sensitive to the concentration of water containing liquid surrounding the fibre. POFBGs have been shown to be highly effective at measuring very small (10-100 ppm) quantities of water (Zhang, et al., 2019).

2.2 Sensor fabrication

For the research presented in this paper, the sensor was created by inscribing a FBG with a nominal Bragg wavelength of 1531 nm in a 10 cm length of single mode, step index PMMA based fibre using a 325 nm HeCd laser and the conventional phase mask approach – see (Webb 2015). The fibre diameter was approximately 95 μm. Because the attenuation of PMMA based POF is around 1dB/cm in this spectral region, the short sensing fibre was glued to a single-mode silica fibre (SMF-28) down-lead for

connection to the interrogation system. The sensor was glued under a small amount of tension (6mε) to an invar plate, either side of the FBG, as shown in Figure 1 and leading to a final Bragg wavelength around 1537 nm. This was done to prevent the fibre from experiencing significant strain induced shifts in the Bragg wavelength. The metal plate holding the fibre was inserted into a 8mm diameter steel tube to protect the sensing fibre from being damaged by contact with the soil. The end of the tube from which the fibre exits was sealed with glue, while the far end of the tube was covered with a metallic mesh [0.3 mm holes on a 0.4mm spacing]. The mesh was chosen so as to prevent soil particles from entering the tube and potentially damaging the fibre but to allow free passage of moisture (and drainage of liquid water) to enable the air space within the tube to achieve an equilibrium with the surrounding soil – see Figure 2(a-b).

The POFBG was interrogated using a broad band source [Agilent 83437A] emitting around 50μW across the C-band, with the reflected signal from the POFBG being monitored using an I-Mon 52 USB spectrometer from Ibsen Photonics. This unit provides 512 measurement points across the spectral region 1510-1595 nm. In this study the POFBG sensor was calibrated to measure/predict variations of gravimetric soil water content (w).

Figure 1

Figure 2 (a)

Figure 2 (b)

An important feature of FBG sensors, that can significantly reduce the system cost when many measurement points are required, is the ability to address multiple sensors with a single interrogation system using some combination of wavelength, time or spatial division multiplexing (Yun-Jiang, et al., 1996). A potential disadvantage of such sensors is the cross-sensitivity to temperature and strain. In our device, we effectively removed the sensitivity by fixing the fibre to a rigid metal plate that could not be significantly deformed by the forces likely to be experienced in our experiments. Temperature sensitivity was simply dealt with by separately monitoring the soil temperature (Section 3). Note that in a practical system, a simple solution to the sensor's cross-sensitivity to temperature and strain would be to record a second FBG in the silica fibre inside the sensor housing. This grating would respond to temperature but not to water content, as silica is insensitive to humidity. The two grating responses could be distinguished using wavelength division multiplexing, as was done in a previous sensor used to monitor humidity and temperature (Zhang, 2010).

3. Effect of temperature on the sensor's performance

Whilst the literature shows reasonable agreement over the normalised strain sensitivities of various POFBGs, there is a much greater range of reported values when it comes to temperature. Partly this is because in the early days of the technology, many measurements were made in the open laboratory environment where the humidity was not controlled leading to cross sensitivity issues (Webb, 2015). In such experiments, sensitivities as high as -360 pm $°C^{-1}$ were reported (Liu, et al., 2001). Consequently, we calibrated the temperature response of our sensor using an environmental chamber [Binder KBF 115] under constant humidity. Changes in wavelength were observed and recorded at increasing temperature (shown by T in Figure 3 (a-b)) increments of two degrees of Celsius. Figure 3(a) shows how the

sensor responded to temperature changes at a constant relative humidity of 40%. It can be observed that the sensor's wavelength decreases with increasing temperature (this arises because the negative thermo-optic coefficient of PMMA has a greater contribution to the wavelength shift than the thermal expansion of the fibre). In order to determine a temperature correction factor, for each temperature, the recorded data over the last 10 minutes were used to provide a mean wavelength (Figure 3(b)). Using a linear regression, a temperature correction factor of 0.11 nm per one Celsius increment of temperature with regard to the normal room temperature of 20 °C (as the reference temperature) was determined and applied to the results (Figure 3b).

Figure 3(a)

Figure 3(b)

4. Soil properties

All soil samples used in this study were silica sand (Leighton Buzzard sand), with index data of specific gravity of 2.66, and nominal effective size of 0.63-0.85 mm. A particle size distribution analysis was performed based on (BSI, 1999 (a)) and the results is presented in Figure 4. It is worth noting that from this point onwards the term 'soil' refers to the silica sand that was used in this paper.

Figure 4

Two degrees of compactions 'loosely' and 'normally' compacted, were used throughout the experiments. The following expressions (Equations 2 and 3) were used to determine the soil porosity (n):

$$n = 1 - \frac{\rho_d}{\rho_{solid}} \quad (2)$$

where

$$\rho_{solid} = G_s \times \rho_w \quad (3)$$

and ρ_{solid} is the density of solid particles of soil; ρ_d is the soil density in dry condition; ρ_w is the density of water; G_s is the soil specific gravity (2.66) and n is the soil porosity. Table 1 shows the properties of the soil samples, including their porosity, used in this study.

Table 1

5. Experimental apparatus and soil samples preparation

A standard proctor mould was employed to place and compact the soil samples in three equal layers. A minor modification was applied to the mould wherein the base plate of the mould was completely sealed to the cylinder in order to prevent any water leakage particularly for higher water content (Figure 5). The soil samples were oven dried at 105°C overnight and then kept in the laboratory environment for at least 24 hours until the soil moisture and temperature equalised with the laboratory condition. In this study, we refer to this state as the '*dry soil*' condition. The soil samples in the laboratory were initially mixed at *dry soil* condition to ensure the individual components were as homogenous as practically possible. In order to generate the predefined different gravimetric water content (w_0'), tap water was added using a pipette to the *dry soil* and the soil-water mixture was mixed for a duration of 3 minutes using an electrical stand mixer. It should be noted that a fixed amount of *dry soil* was measured for the samples prepared in this study while the amount of the added water was different; as we wanted to keep the soil dry unit weight constant in each sets of experiments.

Two sets of experiments were carried out based on the level of compactions. The first set was compacted according to BS 1377-4 standard (BSI, 1999 (b)), using a standard proctor, we refer to this as the 'normally' compacted set or set (i). Set (ii) of the experiments were carried out under a loose compaction condition.

After the soil was sufficiently mixed with water, then the samples in set (i) and (ii) were compacted in three equal layers in which each layer received 27 blows. A 2.5 kg and 0.5 kg rammer were used for compaction purpose in set (i) and (ii), respectively. For both experiments, drop height was 30 cm and the volume of the mould was kept constant at 1000 cm^3. Various predefined soil water contents (w_0') were tested per each set of experiments (a summary of this information is presented in Table 2). To ensure consistency of the experiments and their results, each test, for both sets, were repeated three times.

The POFBG sensor was inserted into the soil sample to a depth of 5cm (Figure 5) and the sample was carefully wrapped using an airtight cling film to minimise evaporation during each test. The soil temperature varied between tests in the range 20 to 23 degrees ºC due to room temperature fluctuations. In each test, the soil temperature was recorded and the POFBG temperature calibration correction applied. In order to evaluate the sensor's performance, after each test, the moist soil sample was used to calculate the gravimetric soil water content (w') using the oven-drying method (Table 3) (BSI, 1999 (a)).

Table 2

Figure 5

6. Initial sensor response to dry-wet-dry soil environment

As an initial test of the sensor response, the sensor was moved between dry and wet ($w_0' = 20\%$) in one of the samples in set (i), with the results being presented in Figure 6. In this graph, changes of the wavelength are presented versus time. Immediately after the first dry phase, when the sensor was introduced to the wet soil, it can be observed that the measured wavelength increases towards a limiting value of 1537.82nm. This somewhat exponential response with a time constant of 1.5 hours is typical response of the sensor to a step change in humidity. The slow response is due to the time needed for the air space in the sensor tube to escape and the polymer fibre itself to reach equilibrium with the soil mixture. Depending on the application, the sensor can be redesigned to have a shorter response (as short as few minutes or less) by reducing the volume of airspace around the fibre (Zhang, et al., 2011). From t_1 the sensor's wavelength starts to rise once again until it reaches a new position at t_2. This second increase was unexpected, but we attribute it to a gradual movement of water through soil voids due to gravity. We expect this would be less pronounced for the normally compacted samples given the higher porosity of loosely compacted soil facilitates the gradual water movement through the initially homogenous soil medium resulting in a variation of water content with depth and therefore a change in the measured wavelength. After t_2, the sensor has reached a stable stage and did not show any significant subsequent changes. The POFBG sensor was removed at t_3 and placed in a dry soil sample again and it can be seen that there is a noticeable drop in the sensor's wavelength from t_3 until it gets to a steady wavelength which is almost equal to the recorded wavelength in the first dry phase. The slight difference between two dry phases is due to the change in the soil temperature (from 20 ºC to 21 ºC) over the period of the experiment (≈ 9 hours).

Figure 6

7. Results and discussion

7.1 Sensor response to changes in water content and in degree of compaction

Samples with different water contents ranging from 0.5% to 20% for the loosely compacted and from 0.5% to 18% in the normally compacted soils were prepared in a controlled laboratory environment. The effect of different water content in addition to the impact of compaction on the sensor's wavelength response, were investigated. Each single test was repeated at least three times to reduce potential errors in the test procedure, or data collection. In both sets (set i and ii) samples were compacted up to nearly saturation condition. Therefore, it was impractical to perform the standard compaction test above 18% water content, as the samples become fully saturated at water content of 21% (Table 1 and Equation 6). Results of all the experiments for both sets, as well as their corresponding water content values (determined using the oven-drying method w'), are shown in Table 3. It should be noted that the temperature correction factor of 0.11 nm per one Celsius increment of temperature has been applied to all recorded wavelengths. These values were obtained from the average sensor's response in its last 15 minutes per each sample.

Table 3

Figure 7 and 8 demonstrate the sensor's response to various soil water contents for all samples in set (i) and (ii), respectively. Each test was repeated three times and all three measurements per each water content in set (i) and (ii) are presented in Figure

7 and 8, respectively. It is evident that the sensor is able to detect small changes in soil water content even as low as 0.5%.

Out of a total of 36 tests, data from three tests were considered out of the range and therefore excluded from the rest of analysis. These corresponded to those samples in set (i) where $w_0' = 0.5$ and in set (ii) where w_0' =0.5 and 1%, (shown by red filled circle symbols in Figure 7 and 8). The decision to consider these out of the range were justified by comparing the values with those measured by the oven-drying method (w'). The most likely reason for these differences is loss of added water during sample preparation.

Figure 7

Figure 8

Using the mean values of each test, the sensor's sensitivity to soil water content were estimated as 0.011±0.001nm/percent and 0.0081±0.0003nm/percent for normally and loosely compacted samples, respectively. Additionally, standard error values in water contents were calculated as $\frac{0.009}{0.011} = 0.82\%$ for loosely and $\frac{0.005}{0.008} = 0.63\%$ for normally compacted samples. The relatively low values of standard error indicate consistency of the obtained data throughout the test and demonstrate the ability and accuracy of the developed sensor for soil water content measurement.

Additionally, it can be observed that in both sets of experiments we can establish a linear relationship between soil water content (w) and the sensor's wavelength (λ) which can be expressed by Equation 4 and 5 for loosely and normally compacted

samples, respectively. This further demonstrates the suitability of the sensor for use in this application.

$$w(\%) = \frac{\lambda + 0.11\,(T_{soil} - 20) - 1537.72}{0.01} \times 100 \quad \text{in Loosely compacted samples} \tag{4}$$

$$w(\%) = \frac{\lambda + 0.11\,(T_{soil} - 20) - 1537.64}{0.01} \times 100 \quad \text{in Normally compacted samples} \tag{5}$$

Note in the above equations T_{soil} is in degree of Celsius and these equations are valid to predict the soil water content up to nearly saturation condition in the sandy soils presented in Table 1.

For comparison, the sensor's response to changes of water content for both compaction conditions are shown in Figure 9. The sensor's wavelength (λ) in set (i) is smaller than those of set (ii) which can be explained by the smaller porosity in the normally compacted samples compared to the loosely compacted ones and the fact that in more compacted soil, where the porosity is lower, less water content (soil moisture) is required to make the sample fully saturated. Using Equation 6, the degree of saturation for all samples with different moisture content are calculated and presented in Figure 10. This equation explains the relationship between soil water content (w), soil void ratio (e), degree of saturation S_r and specific gravity (G_s):

$$S_r \times e = w \times G_s \tag{6}$$

Figure 9

Figure 10

7.2 Evaluation of the sensor's performance

For comparison and completeness, a commercial soil water content measurement sensor, the SM150 probe (Figure 11) was used to measure the volumetric soil water content (θ) in the samples tested above. The probe measures volumetric soil water content by responding to changes in the apparent dielectric constant of the moist soil (Delta-T Devices, 2017). The probe was placed in 4 different locations of the sample in close proximity to and at the same depth where the POFBG sensor was buried. Table 4 shows the measured data by the Probe in a number of the tests for the normally compacted samples. The Probe measurement was recorded when the POFBG sensor reached an equilibrium and a constant wavelength was observed.

Figure 11

Table 4

In Table 4 there are no data for soil water content of 0.5% and 1% as the probe was not sensitive to any soil water content less than 3%. An average of the 4 readings by the probe was calculated and converted to gravimetric soil water content using Equation (1c) and then compared with the oven-drying method (w'), as well as the POFBG sensor predictions (Equation 5) – results are presented in Table 5. Both absolute and percentage errors using the two different measurement tools with respect to the oven-drying method (w') are calculated and presented. Error_1 and Error_2 are the absolute error for water content measured by POFBG (Equation 5) and the probe, respectively. Whilst the percentage error (%) value provides a base for relative

comparison, the absolute error offers a better context for the error in this case since they can provide clearer and direct knowledge of the expected accuracy in the measurements.

Generally, the probe underestimates the gravimetric water content and in particular for low water content where there is a significant percentage error ($> 60\%$). The probe was not able to measure soil water content less than 3%. Additionally, it is worth noting that the corresponding absolute error (mean error) is not within the approximately 3% water content error that is normally considered as an accuracy range of soil water content sensors (Curioni, et al., 2018 a). On the other hand, it can be seen from Table 4 that the average percentage error predicted by Equation 5 is less than 9% and the corresponding absolute value is less than 1.5%.

Table 5

Summary and conclusions

Continuous monitoring of changes in ground conditions by measuring the variations of different ground properties such as water content is vital to analyse the stability of the ground and geotechnical assets which facilitates prediction of their deterioration processes. Soil water content is linked with many critical properties of soils including its strength. There are several techniques available to measure soil water content however, they each suffer from a number of drawbacks ranging from high costs to lack of accuracy. This motivated the authors to develop a resilient and novel polymer optical fibre Bragg grating (POFBG) sensor to accurately measure soil water content. In this study, for the first time, the sensitivity of a fibre Bragg grating (FBG) sensor fabricated in Polymer Optical Fibre (POF) to soil water content was investigated. We

focused on calibrating the POFBG sensor to detect small changes of soil water content rather than the absolute value since variation of the soil water content over time is more critical for geomechanical behaviour of soils. The sensor was properly packaged and buried vertically in a sets of sandy soil samples. The effect of soil temperature on the sensor's response was considered, and a temperature correction factor was determined and applied to all measurements.

The sensor was tested at two different compaction soil conditions of 'loosely' and 'normally' compacted soils and its sensitivity and response to the various values of gravimetric soil water content was investigated. The proposed sensor showed ability to detect changes, even as low as 0.5%, in soil water content which is crucial to monitor geostructures and ground conditions in general. Additionally, the results showed that the sensor is highly sensitive to different soil porosity. It was observed that the relationship between the water content and sensor's wavelength in both compaction conditions is linear which can facilitate the estimation of soil water content up to nearly saturation condition for each soil compaction.

Moreover, the accuracy, reliability and advantages of the sensor's prediction was evaluated by comparing its prediction with commercial soil water content probe (SM150). The measurements by both sensing devices were assessed against the oven-drying method using absolute and percentage error. The comparison results indicated that the developed POFBG sensor's prediction and its sensitivity to water content variation is more accurate than the commonly used commercial probe with mean absolute error of 1.21%.

The proposed sensor in this study can be developed and employed in geo-structures as an early-warning system for monitoring geotechnical assets to detect any changes caused by changes in soil water content (e.g. due to extreme weather condition or

leaking pipe). The use of the POFBG sensor will facilitate in-situ measurement allowing for continuous monitoring of change of water content at multi points and in most cases will eliminate the need for the long and tedious sampling process. Integrating the data collected from this sensor with other key parameters of soil strength will provide a comprehensive picture of the system (soil and infrastructure) where, currently such integrated system does not exist. The integrated model can provide adequate information on structural integrity and stability of the system thereby enabling the decision makers to prevent or tackle potential problems.

However, the sensor's performance should be further investigated by conducting additional laboratory and field trials including different soil types (e.g. clay, clayey sand) and soil properties (e.g. different compaction conditions) to ensure its reliability. The response time of the sensor should also be re-designed and shortened for those applications where small changes of water content in a short time is critical. The current response time of the sensor is suitable for those applications where long-term dynamic monitoring of the ground water table is required for their maintenance such as slopes stability and ground water table variation monitoring. Furthermore, the sensor's stability in longer time from few days to few months needs to be tested in the laboratory as well as in the field.

Acknowledgement

Moura Mehravar would like to thank the Aston Institute of Materials Research (AIMR) for financial support. Hanrui Yang gratefully acknowledges a visiting scholarship supported by the Chinese Scholarship Council. The authors would like to thank Prof Gang-Ding Peng of the University of New South Wales for supply of the polymer fibre.

References:

Bryson, L. S., Jean-Louis, M. & Gabriel, C., 2012. Determination of in situ moisture content in soils from a measure of dielectric constant. *International Journal of Geotechnical Engineering ,* Volume 6, pp. 251-259.

BSI, 1999 (b). *Compaction related tests.* London, BS1377-4.

BSI, 1999 (a). *Methods of tests for soils for civil engineering purposes. Classification tests.* London.

Byoungho, L., 2003. Review of the present status of optical fibre sensors. *Optical Fiber Technology ,* 9(2), pp. 57-79.

Clarke, B. G. et al., 2017. *A decision support system to proactively manage subsurface utilities.* London, In proceedings of the international symposia for next generation infrastructure .

Curioni, G. et al., 2018 b. Extending TDR Capability for Measuring Soil Density and Water Content for Field Condition Monitoring. *Journal of Geotchnical and Goeenvironmental engineering (ASCE),* 144(2), pp. 1-15.

Curioni, G. et al., 2018 a. Time domain reflectometry (TDR) potential for soil condition monitoring of geotechnical assets. *Canadian Geotechnical Journal,* Volume 56, pp. 942-955.

Delta-T Devices, 2017. *User Manual for HH2,* Cambridge: Delta-T Devices Ltd.

Du, H. et al., 2016. An ontology of soil properties and processes. In Semantic Web-Iswc 2016, Pt Ii.

Gong, H. et al., 2019. Advances in fibre optic based geotechnical monitoring systems for underground excavations. *International Journal of Mining Science and Technology ,* 29(2), pp. 229-238.

Gunn, D. A. et al., 2015. Moisture monitoring in clay embankments using electrical resistivity tomography. *Construction and Building Materials ,* Volume 92, pp. 82-94.

Harbach, N. G., 2008. *Fibre Bragg gratting in polymer optical fibres,* Lausanne (EPFL).

Huang Chien, A. B., Wang, C. C., Lee, J. T. & Ho, Y. T., 2016. Application of FBG-based sensors to ground stability monitoring. *Journal of Rock Mecanics and Geotechnical Engineering,* Volume 8, pp. 513-520.

Huang, A. B., Wang, C. C., Lee, J. T. & Ho, Y. T., 2016. Application of FBG-based sensors to ground stability monitoring. *Journal of Rock Mechanics and Geotechnical Engineering ,* Volume 8, pp. 513-520.

Huisman, J. A., Hubbard, S. S., Redman, J. D. & Annan, A. P., 2003. Measuring soil water content with ground penetrating radar. *Vadoze zone journal ,* 2(24), pp. 476-491.

Liu, H. Y., Peng, G. D. & Chu, P. L., 2001. Thermal tunning of polymer optical fibre Bragg grating. *IEEE Photonics Technical letter,* Volume 13, pp. 824-6.

Lopez Aldaba, A. et al., 2018. Comparison between Capacitive and Microstructured Optical Fiber Soil Moisture Sensors. *Applied Science ,* 8(9), pp. 1-12.

Mehravar, M., Yang, H., Zhang, W. & Webb, D., 2019. *Ground-water monitoring using polymer optical fibre Bragg gratings.* s.l., In Seventh European Workshop on Optical Fibre Sensors, International Society for Optics and Photonics.

Mitchell, J. & Soga, K., 2005. *Fundamentals of soil behaviour.* s.l.:John Wiley and Sons, Inc., Hoboken, NJ, 557 pp.

Pritchard, O. G., Hallet, S. H. & Farewell, T. S., 2014. Soil impacts on UK infrastructure: Current and future climate. *Proc. Ins. Civ. Eng. Eng. Sustainability,* pp. 170-184.

Robinson, D. A. et al., 2008. Soil moisture measurement for ecological and hydrological watershed-scale: a review. *Vadose zone journal,* 7(1), pp. 358-389.

Robock, A., 2014. Hydrology, floods and drought: Soil moisture. *In Encylopedia of atmospheric science ,* Volume 2nd edition , pp. 232-239.

Soga, K. et al., 2015. The role of distributed sensing in understanding the engineering performance of geotechnical structures. *Proceedings of the ICE - Geotechnical Engineering fro Infrastructure and Development ,* pp. 13-48.

Webb, D. J., 2015. Fibre Bragg gratting sensors in polymer optical fibres. *MEasurement Science and Technology,* Volume 26, p. 092004.

Yun-Jiang, R. et al., 1996. Simultaneously spatial-, time-, and wavelength-division multiplexed in-fiber Bragg grating sensor network. In: K. Alan D & D. John P, eds. *Distributed and Multiplexed Fiber Optic Sensors VI.* s.l.:International Society for Optics and Photonics, pp. 23-30.

Zhang, C. et. al., 2010. Optical fibre temperature and humidity sensor. *Electronics Letters,* 46(9).

Zhang, W., J, W. D. & Peng, G. D., 2011. *Imprived time response for polymer fibre Bragg grating based humidity sensors.* Ottawa (CA), 21st International COnference on Optical Fibre Sensors (OFS21).

Zhang, W. & Webb, D., 2014. Humidity responsivity of poly9methyl methacrylate)-based optical fibre Bragg grating sensors. *Optic letters ,* Volume 39, pp. 3026-3029.

Zhang, W. et al., 2019. Water content detection in aviation fuel by using PMMA based optical fiber grating. *Sensors and Actuators B: Chemical,* Volume 282, pp. 774-779.

List of figures:

Figure 1: Sensor construction. POF length = 10 cm, with 5mm POFBG at centre. Invar support dimensions = 60x6x3 mm.

Figure 2 (a): The POFG sensor packaging (outer diameter = 8mm).

Figure 2 (b): Metallic mesh end cover to protect the sensor.

Figure 3(a): The sensor's sensitivity to temperature changes in a constant relative humidity of 40%

Figure 3(b): The sensor's response to temperature changes in a constant relative humidity of 40%

Figure 4: Soil particle size distribution curve (sieve analysis test)

Figure 5: Standard proctor mould and soil sample

Figure 6: The measured/reflected wavelength from the POFBG sensor for 20% soil water content in the loosely compacted soil

Figure 7: POFBG response to different gravimetric soil water content in the normally compacted soil samples

Figure 8: POFBG response to different gravimetric soil water content in the loosely compacted soil samples

Figure 9: Comparison of the sensor's response in normally and loosely compacted samples

Figure 10: Saturation degree (%) at each water content in loosely and normally compacted samples

Figure 11: SM150 probe to measure the volumetric soil water content

List of tables:

Table 1: soil properties

Table 2: parameters for each set of experiments used in this study

Table 3: Results of all the tests for both sets (i) and (ii)

Table 4: Measured θ by the probe at four different locations in Normally compacted samples

Table 5: Validation of the SM150 probe measurements for a selected number of normally compacted samples in partially saturated samples

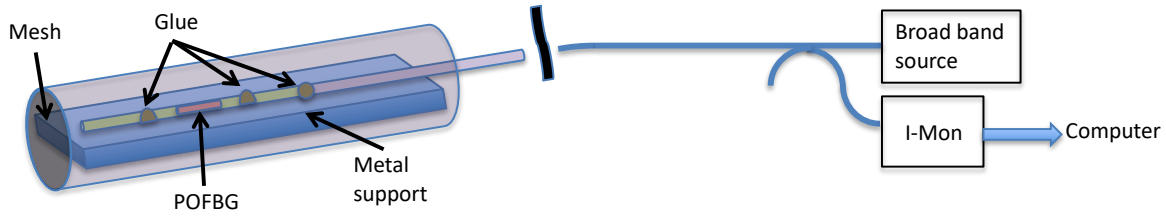

Figures 1: Sensor construction. POF length = 10 cm, with 5mm POFBG at centre. Invar support dimensions = 60x6x3 mm.

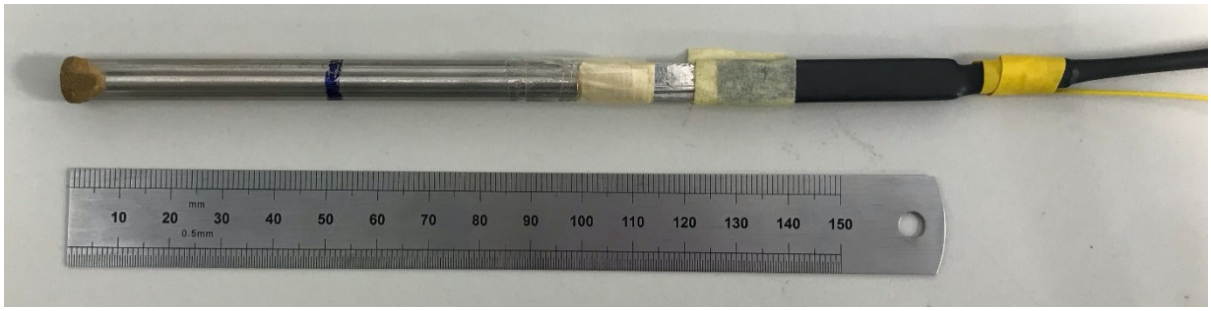

Figure 2 (a): The POFG sensor packaging (outer diameter = 8mm).

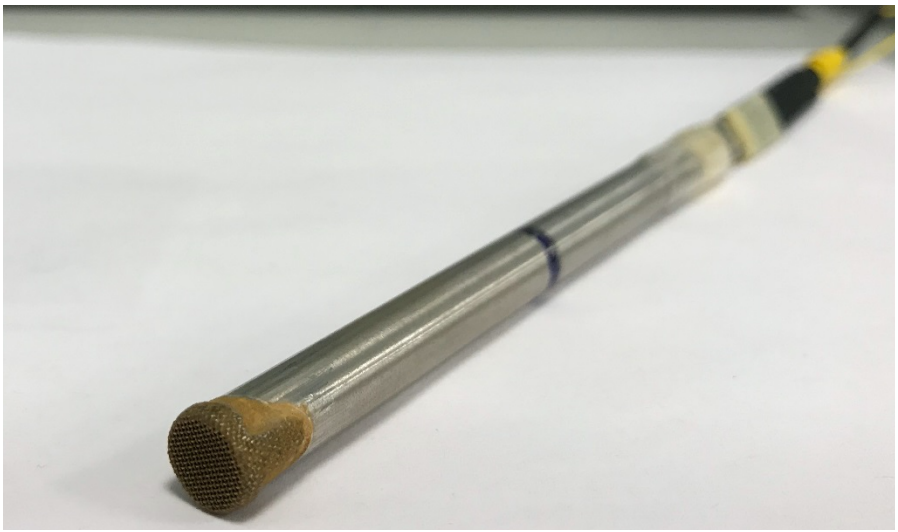

Figure 2 (b): Metallic mesh end cover to protect the sensor.

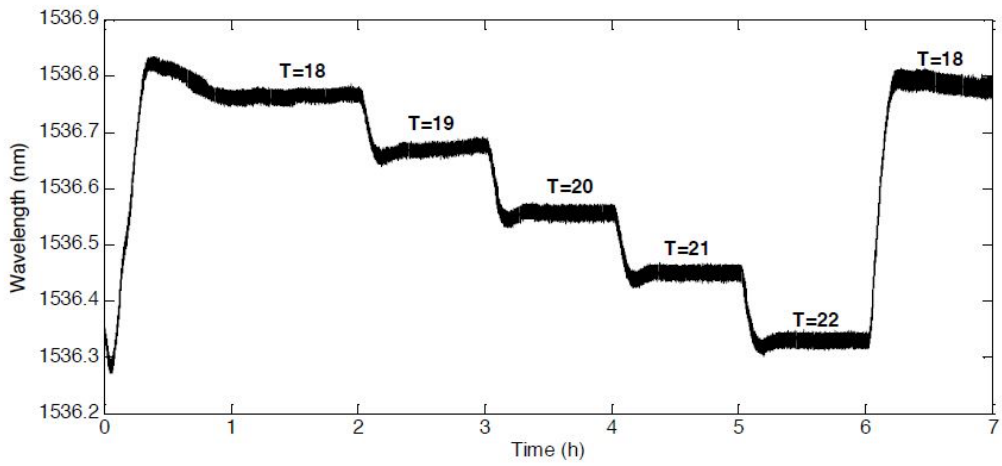

Figure 3(a): The sensor's sensitivity to temperature changes in a constant relative humidity of 40%

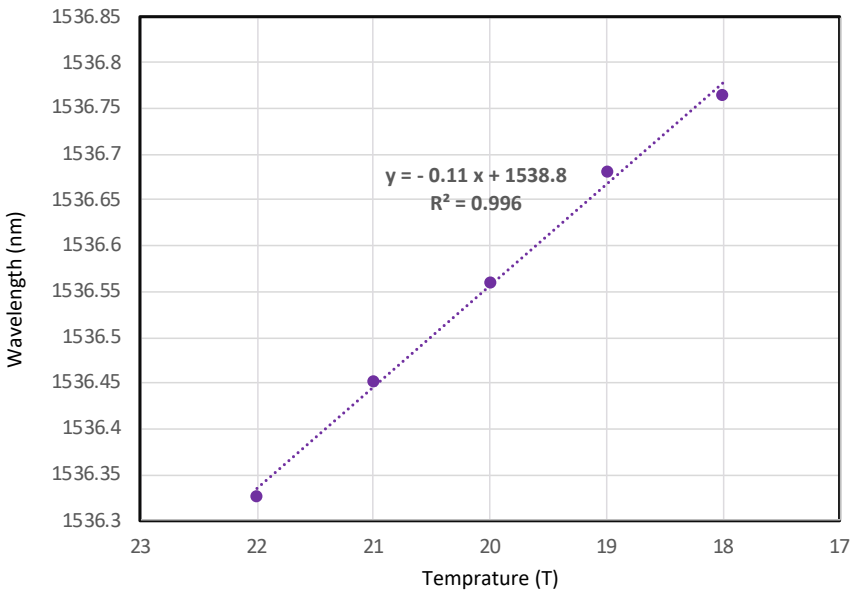

Figure 3(b): The sensor's response to temperature changes in a constant relative humidity of 40%

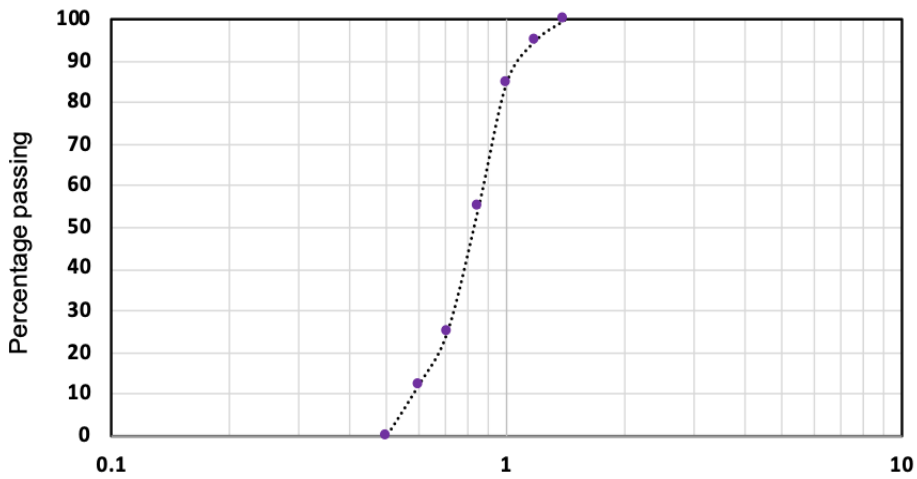

Figure 4: Soil particle size distribution curve (sieve analysis test)

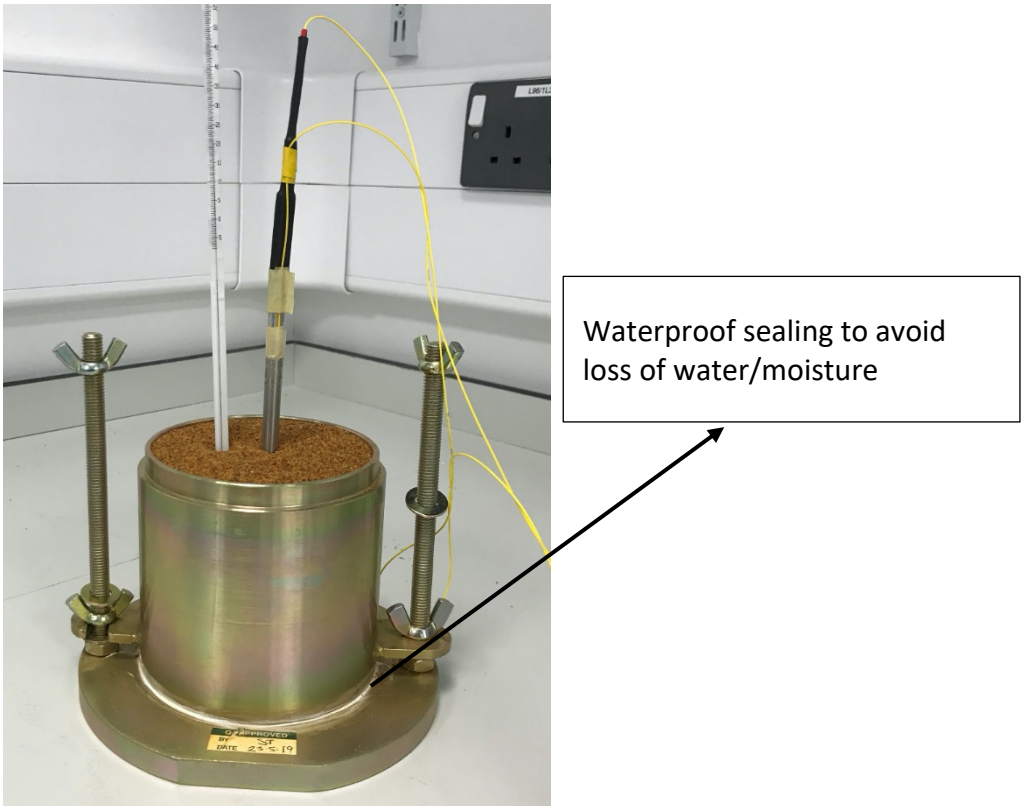

Figure 5: Standard proctor mould and soil sample

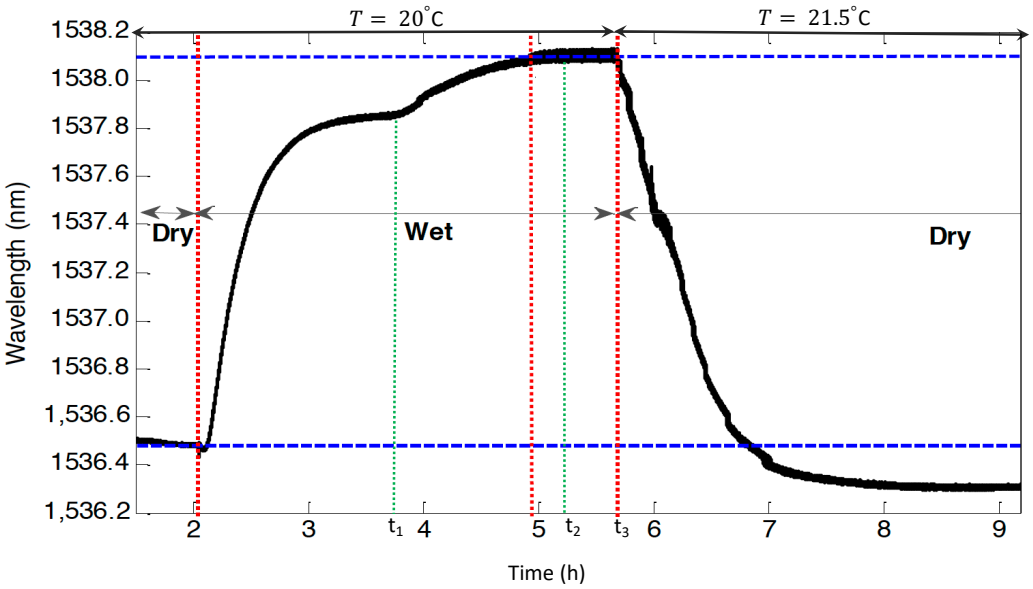

Figure 6: The measured/reflected wavelength from the POFBG sensor for 20% soil water content in the loosely compacted soil

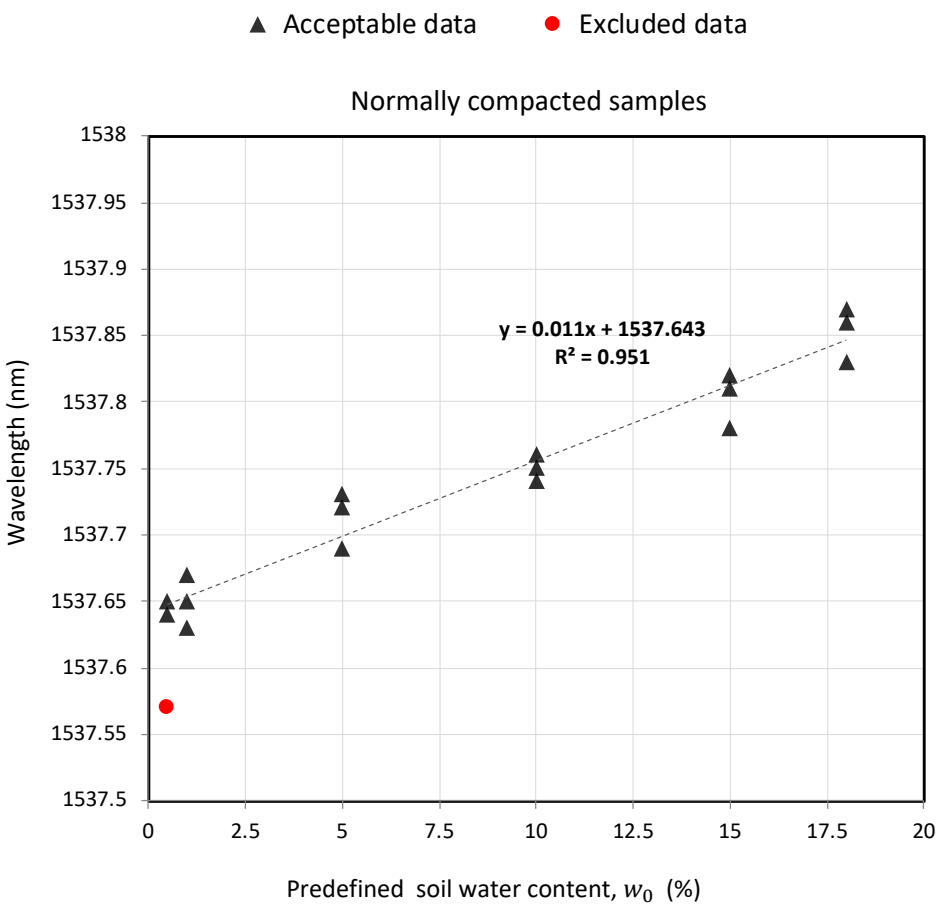

Figure 7: POFBG response to different gravimetric soil water content in the normally compacted soil samples

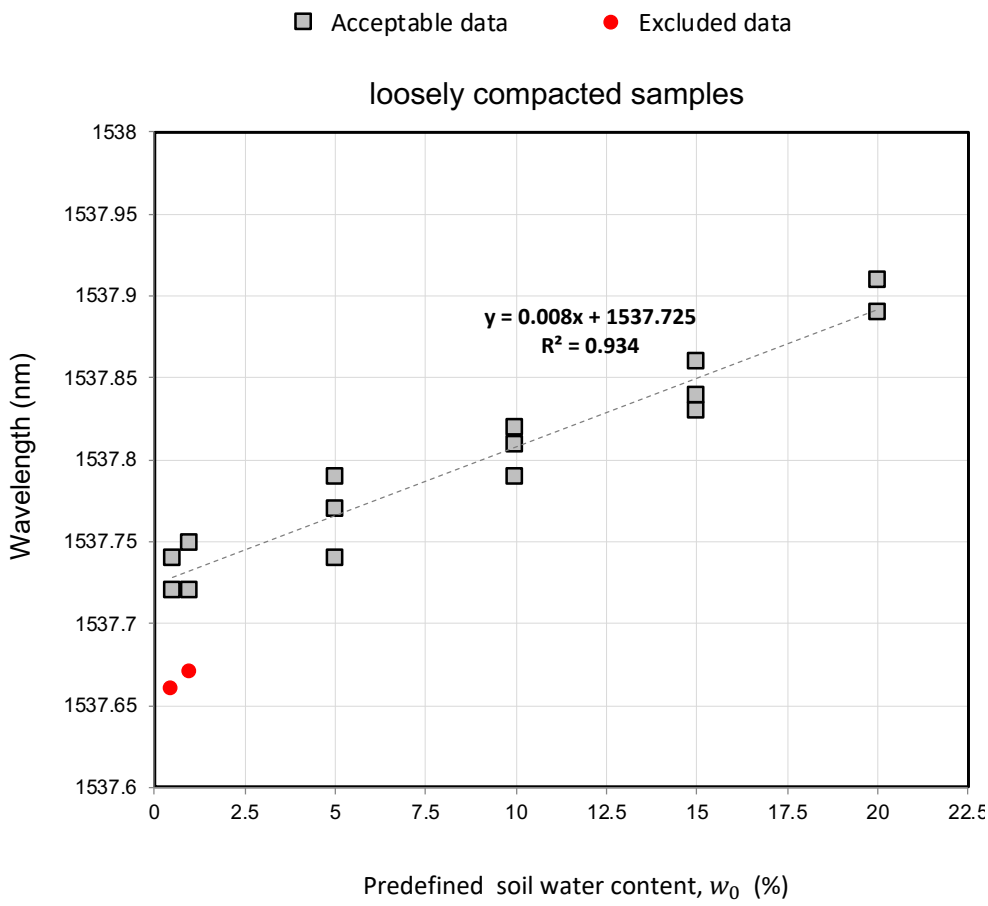

Figure 8: POFBG response to different gravimetric soil water content in the loosely compacted soil samples

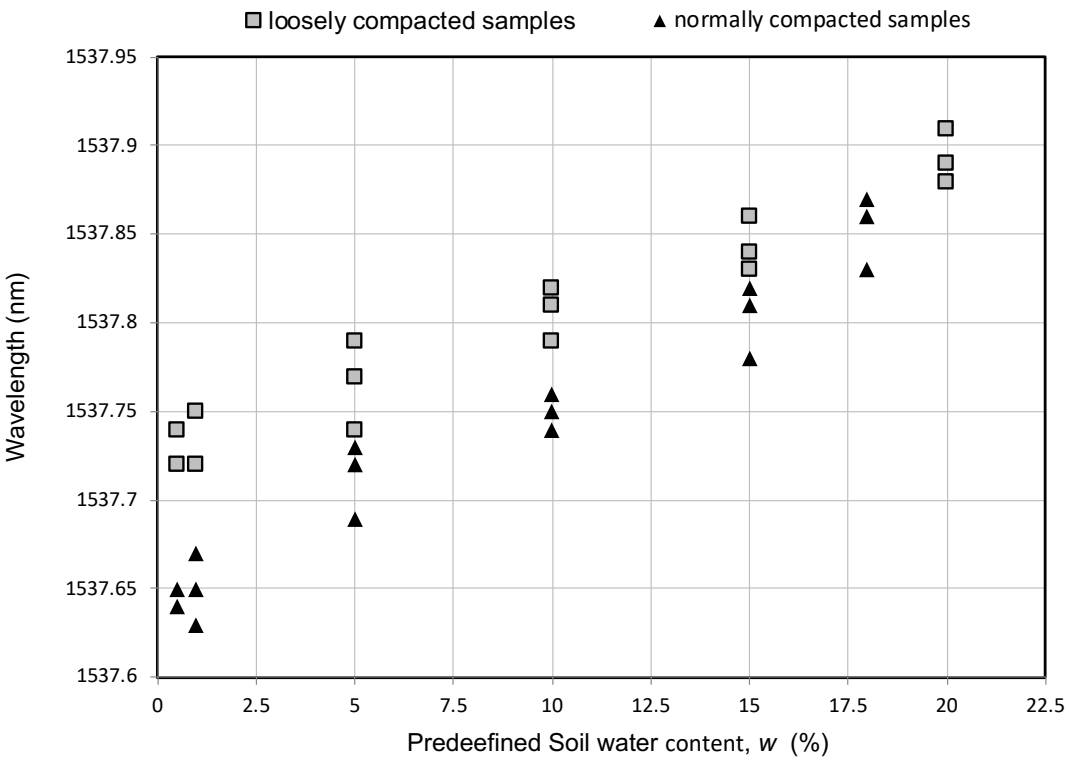

Figure 9: Comparison of the sensor's response in normally and loosely compacted samples

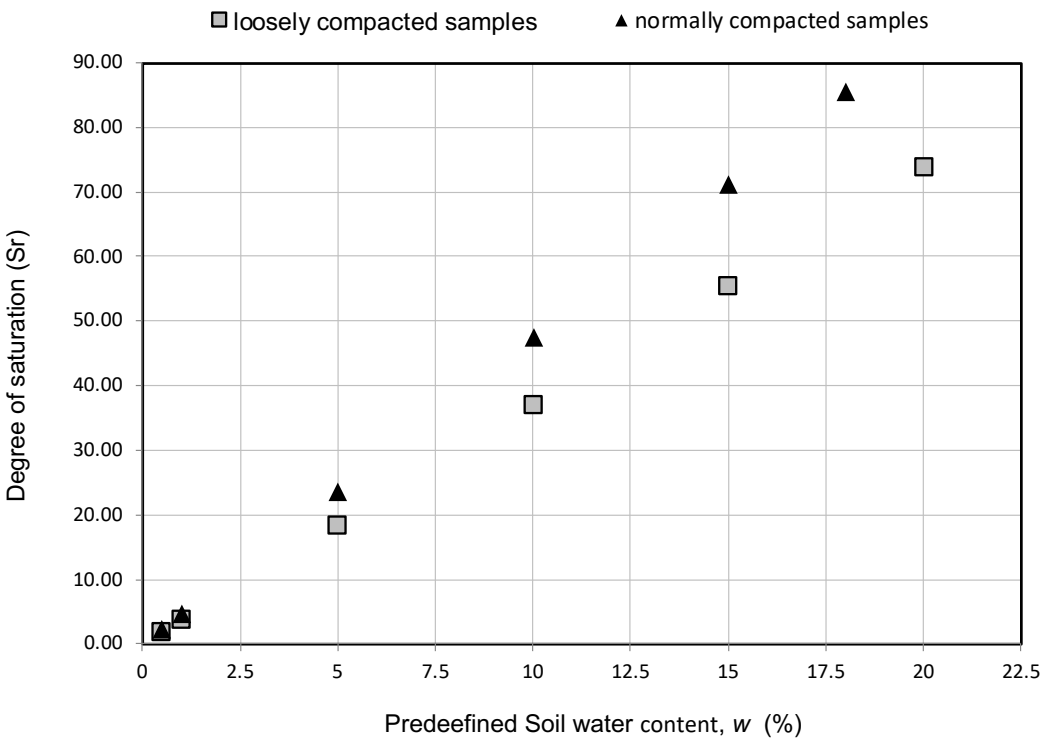

Figure 10: Saturation degree (%) at each water content in loosely and normally compacted samples

Figure 11: SM150 probe to measure the volumetric soil water content

Table 1: soil properties

Test	Bulk (dry) density (g/cm^3)	Porosity (n) (%)
Normally compacted (standard proctor)	1.69	36
Loosely compacted	1.55	42

Table 2: parameters for each set of experiments used in this study

Test	No. of layers	No. of blows per layer	Hammer weight (kg)	Drop height (cm)	Proctor standard mould volume (cm^3)	Predefined soil water content w_0' (%)
Set (i): normally compacted (standard proctor)	3	27	25	30	1000	0.5, 1, 5, 10, 15, 18
Set (ii): Loosely compacted	3	27	5	30	1000	0.5, 1, 5, 10, 15, 20

Table 3: Results of all the tests for both sets (i) and (ii)

	Set (i): normally compacted			Set (ii): loosely compacted		
Test number	Predefined soil water content w_0' (%)	Recorded wavelength (nm)	Reference w' (%) by oven-dried method	Predefined soil water content w_0' (%)	Recorded wavelength (nm)	Reference w' (%) by oven-dried method
1	0.5	1537.65	0.47	0.5	1537.72	0.48
2		1537.64	0.48		1537.66	0.38
3		1537.57	0.39		1537.74	0.46
1	1	1537.63	0.95	1	1537.67	0.79
2		1537.67	0.96		1537.72	0.92
3		1537.65	0.97		1537.75	0.93
1	5	1537.69	4.87	5	1537.77	4.83
2		1537.72	4.89		1537.79	4.84
3		1537.73	4.91		1537.74	4.81
1	10	1537.76	9.86	10	1537.81	9.85
2		1537.75	9.78		1537.79	9.77
3		1537.74	9.73		1537.82	9.84
1	15	1537.78	14.40	15	1537.83	14.78
2		1537.81	14.52		1537.84	14.81
3		1537.82	14.54		1537.86	14.82
1	18	1537.83	17.82	20	1537.91	19.64
2		1537.87	17.87		1537.89	19.63
3		1537.86	17.74		1537.88	19.64

Table 4: Measured θ by the probe at four different locations in Normally compacted samples

Reference w' (%) by oven-dried method (gravimetric water content)	θ measured by the SM150 probe (%) (volumetric water content)
4.87	3.1, 3.1, 2.9, 3.2
9.86	5.6, 5.7, 5.5, 5.3
14.40	20.6, 20.9, 20.3, 20.2
17.82	27.4, 26.8, 28.3, 27.5

Table 5: Validation of the SM150 probe measurements for a selected number of normally compacted samples in partially saturated samples

Soil sample condition	Reference w' (%) by oven-dried method	w (%) estimated by POFBG (Equation 5)	Error $_1$ *	w by the SM150 probe (%)	Error$_2$ *
Normally compacted soil	4.87	5	0.13 [2.67]	1.82	-3.00 [62.24]
	9.86	12	2.14 [21.7]	3.27	-6.56 [66.73]
	14.40	14	0.40 [2.8]	12.13	-2.27 [15.76]
	17.82	19	1.18 [6.62]	16.27	-1.48 [8.34]
Mean Error	-	-	1.21[8.44]	-	-3.33 [38.26]

* Values in square brackets are % error.